Electronic Supplementary Material (ESI) for Faraday Discussions.

Effect of crystallite size on the performance and phase transformation of Co_3O_4/Al_2O_3 catalysts during CO-PrOx - An *in situ* study

Thulani M. Nyathi,[a] Nico Fischer,[a] Andy P. E. York[b] and Michael Claeys[a,*]

Magnetism

Ferromagnetism: Materials that exhibit this behaviour are attracted by an applied magnetic field (symbol: **H**, units: **T** (Tesla) or **kOe** (kilo-Oersted)) via the parallel alignment of neighbouring electron spins forming microscopic regions called magnetic domains.[1-3] Upon removal of this external field, the material or a fraction of it, remains magnetised and the observed magnetisation is called remnant magnetisation (**M_{rem}**). This behaviour is a result of the strong coupling between the neighbouring electron spins.[3] Ferromagnetism is temperature-dependent and material-specific therefore, there exists a critical temperature above which ferromagnetic materials lose their ferromagnetic character and become paramagnetic. This critical temperature is called the Curie temperature (**T_C**). The loss in ferromagnetic behaviour above T_C is a result of an increase in the thermal energy which mitigates the strong interaction between neighbouring spins.[3]

Superparamagnetism: This is a special case of ferromagnetism whereby small crystallites (normally in the nanometre range) completely lose their magnetisation upon removal of the external field.[4] Superparamagnetism is crystallite size-dependent and material-specific therefore, there exists a critical crystallite size whereby a ferromagnetic sample will display superparamagnetic behaviour.[4]

Antiferromagnetism: Is almost like ferromagnetism except that the neighbouring spins align themselves in opposite directions in the presence of an applied field.[1-3] Antiferromagnetic behaviour is also temperature-dependent and the critical temperature below which antiferromagnetic behaviour can be observed is called the Néel temperature (**T_N**). Above this critical temperature, antiferromagnetic materials also become paramagnetic.[3]crystallite size in the absence of H_2.[14-16] To the best of our knowledge, studies investigating the effect of crystallite size on the catalytic activity of Co_3O_4 during CO-PrOx have not been reported.

Magnetometer calibration

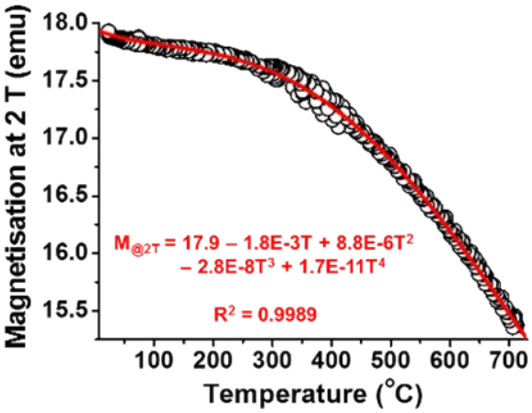

Figure S.1: Sample magnetisation of a 0.1 g pre-reduced metallic cobalt sample as a function of temperature.

$$m_{Co\ formed}\,(g) = \frac{M_{experimental} \cdot 0.1\ g}{M_{calibration}} \qquad Equation\ S.1$$

$$Degree\ of\ reduction\ (\%) = \frac{m_{Co\ formed}}{0.73 \cdot m_{Co_3O_4\ loaded}} \times 100 \qquad Equation\ S.2$$

[a]*Catalysis Institute and c*change (DST-NRF Centre of Excellence in Catalysis), Department of Chemical Engineering, University of Cape Town, Rondebosch 7701, South Africa.* [b]*Johnson Matthey Technology Centre, Sonning Common, Reading RG4 9NH, United Kingdom. *Corresponding author: Michael.Claeys@uct.ac.za*

Where $m_{Co\ formed}$ is the mass of cobalt formed at temperature T_i. $M_{experimental}$ is the sample magnetisation (unit: emu) measured at temperature T_i during the CO-PrOx experiment and $M_{calibration}$ is the magnetisation (unit: emu) measured at temperature T_i during the calibration of the magnetometer with a 0.1 g metallic cobalt sample. $m_{Co_3O_4\ loaded}$ is the initial Co_3O_4 mass loading as determined by EDX.

TEM of fresh catalysts

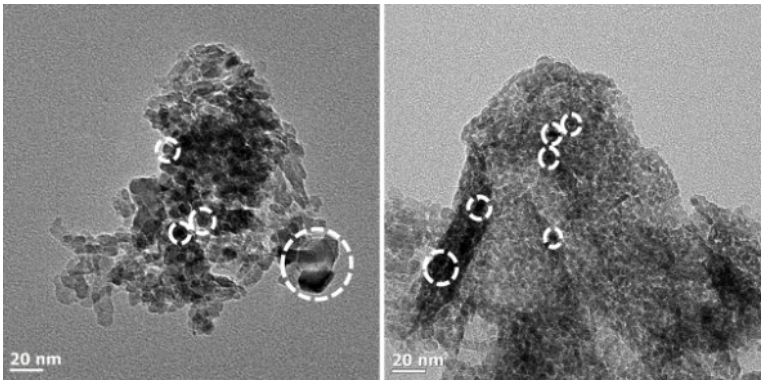

Figure S.2: Selected TEM micrographs of the fresh samples of the supported samples of (***left***) TN_01 and (***right***) TN_05. The white dotted circles show single and/or a cluster of Co_3O_4 crystallites.

In situ characterisation and kinetic data

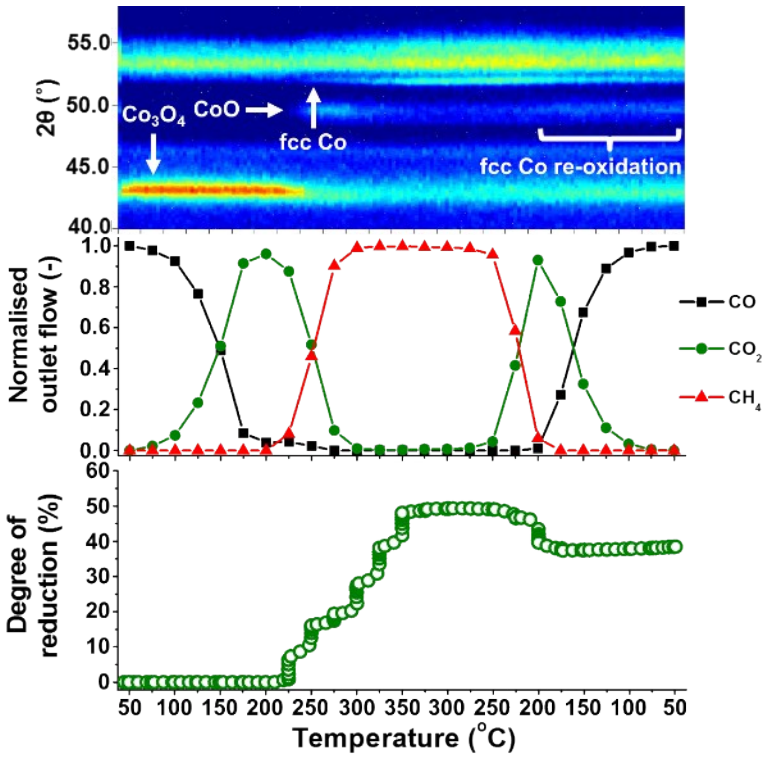

Figure S.3: (***top***) On-top view of the PXRD patterns recorded for TN_02, (***middle***) the normalised outlet flow rates of CO, CO_2 and CH_4, (***bottom***) as well the changes in the degree of reduction calculated from the magnetometer-derived data.

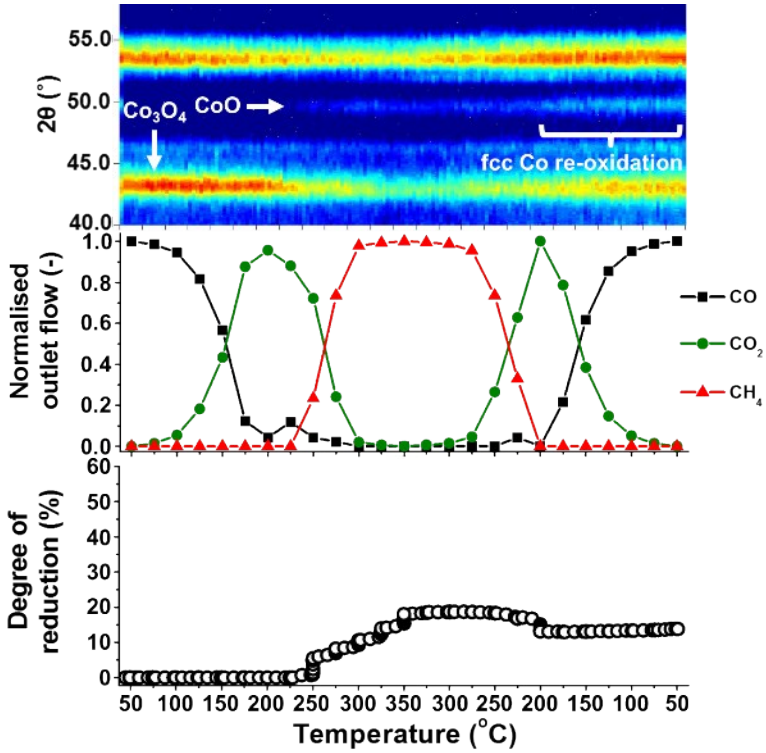

Figure S.4: (***top***) On-top view of the PXRD patterns recorded for TN_03, (***middle***) the normalised outlet flow rates of CO, CO_2 and CH_4, (***bottom***) as well the changes in the degree of reduction calculated from the magnetometer-derived data.

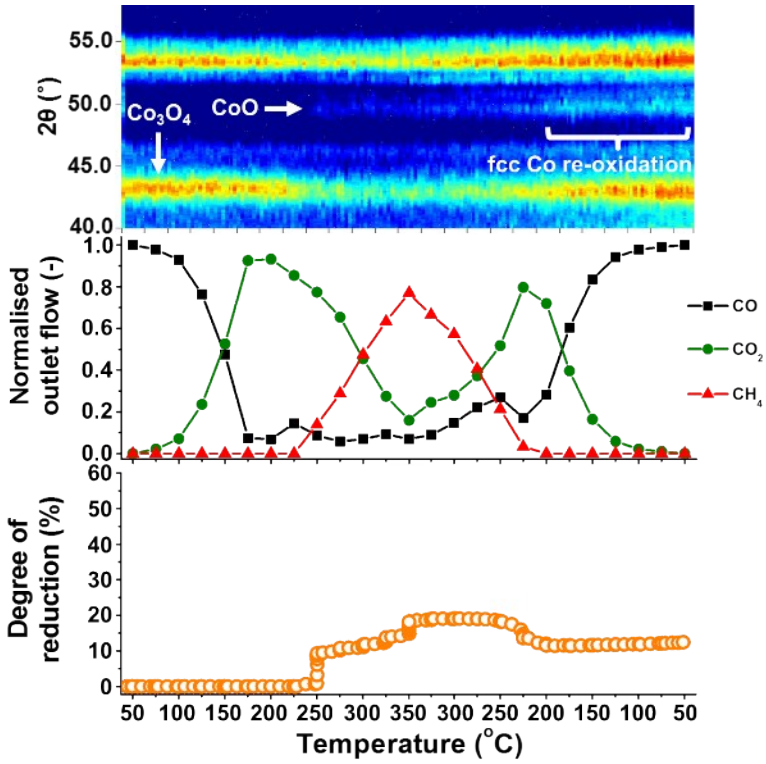

Figure S.5: (***top***) On-top view of the PXRD patterns recorded for TN_04, (***middle***) the normalised outlet flow rates of CO, CO_2 and CH_4, (***bottom***) as well the changes in the degree of reduction calculated from the magnetometer-derived data.

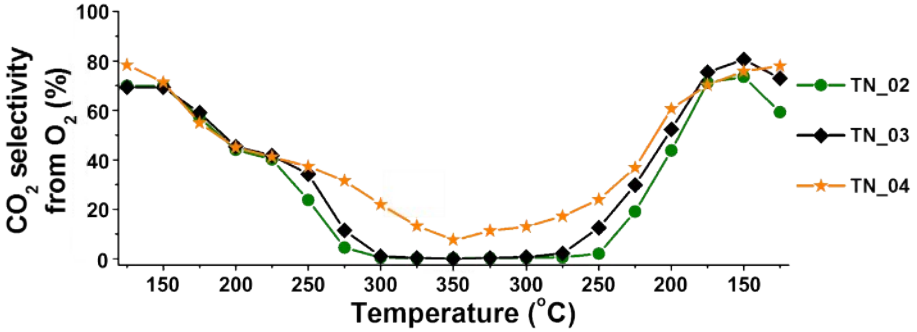

Figure S.6: CO_2 selectivity based on the conversion of O_2 as a function of temperature for the catalysts TN_02 - TN_04.

The normalised outlet flowrates of CO (N_{CO}), CO_2 (N_{CO_2}) and CH_4 (N_{CH_4}), as well as the CO_2 selectivity based on the conversion of O_2 ($S_{CO_2}^{O_2}$) and the surface area-specific CO_2 formation rate (r_{CO_2}) were all calculated using Equations S.1 – S.5. The conversion of H_2 was too low to be accurately measured during the runs, however, it is worth mentioning that the H_2O selectivity based on the conversion of O_2 ($S_{H_2O}^{O_2}$) can be expected to be $100 - S_{CO_2}^{O_2}$.

$$N_{CO} = \frac{n_{CO,\ out}}{n_{CO,\ in}} = \frac{n_{CO_2,\ out} - n_{CH_4,\ out}}{n_{CO,\ in}} \qquad \textit{Equation S.3}$$

$$N_{CO_2} = \frac{n_{CO_2,\ out}}{n_{CO,\ in}} = \frac{n_{CO,\ out} - n_{CH_4,\ out}}{n_{CO,\ in}} \qquad \textit{Equation S.4}$$

$$N_{CH_4} = \frac{n_{CH_4,\ out}}{n_{CO,\ in}} = \frac{n_{CO,\ out} - n_{CO_2,\ out}}{n_{CO,\ in}} \qquad \textit{Equation S.5}$$

$$S_{CO_2}^{O_2}(\%) = \frac{n_{CO_2,\ out}}{2 \cdot \left(n_{O_2,\ in} - n_{O_2,\ out}\right)} \times 100 = \frac{n_{CO,\ in} - n_{CO,\ out} - n_{CH_4,\ out}}{2 \cdot \left(n_{O_2,\ in} - n_{O_2,\ out}\right)} \times 100 \qquad \textit{Equation S.6}$$

$$r_{CO_2}\left(molec_{CO_2}.nm^{-2}.s^{-1}\right) = \frac{n_{CO_2,\ out} \cdot d_{c,\ n} \cdot \rho_{Co_3O_4} \cdot N_A}{6 \cdot m_{Co_3O_4\ loaded}} \qquad \textit{Equation S.7}$$

Where $n_{CO,\ in}$ and $n_{O_2,\ in}$ are the molar gas flow rates of CO and O_2 respectively, entering the reactor under reaction conditions. $n_{CO,\ out}$, $n_{O_2,\ out}$, $n_{CO_2,\ out}$ and $n_{CH_4,\ out}$ are the molar gas flow rates of CO, O_2, CO_2 and CH_4 respectively, exiting the reactor under reaction conditions. $d_{c,n}$ is the average TEM number-based crystallite size assuming no or negligible sintering (in nm), $\rho_{Co_3O_4}$ is the density of Co_3O_4 (in g.nm^{-3}), N_A is Avogadro's number (in molecules per mole) and $m_{Co_3O_4\ loaded}$ is the initial Co_3O_4 mass loading as determined by EDX.

TEM of spent catalysts

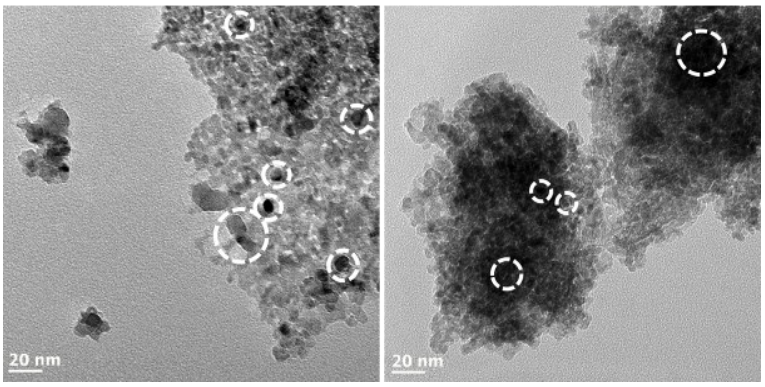

Figure S.7: Selected TEM micrographs of the spent samples of (***left***) TN_01 and (***right***) TN_05. The white dotted circles show single and/or a cluster of Co_3O_4 crystallites.

References

1 Buschow, K. H. J. *Encyclopedia of Materials: Science and Technology*; Amsterdam, Netherlands: Elsevier, 2001; Vol. 5, p. 5021.

2 Kittel, C. *Introduction to Solid State Physics*; London: John Wiley & Sons, Inc., 2009.

3 Serway, R., Jewett, Jr., J. *Physics for Scientists and Engineers with Modern Physics*; Boston: Brooks/Cole, 2014.

4 Dalmon, J. Magnetic measurements and catalysis. In *Catalyst characterisation: Physical techniques for solid materials*; B. Imelik, B. & Verdrine, J., Eds.; New York: Plenum Press; p 585.